

Modeling and Simulation of a Matrix Converter/Induction Motor System

Ibrahim A.M. Abdel-Halim, Hamed G. Hamed, Mohammed E. Elfaraskoury and Ahmed M. Hassan
 Department of Electrical Engineering, Faculty of Engineering, Benha University,
 108 Shoubra St., Cairo, Egypt

Abstract: In this study, a system composed of a matrix converter and an induction motor is modeled and simulated using Matlab/Simulink software package. The modulation techniques used for the matrix converter are Venturini and Optimum Venturini Methods. The variation of motor voltages, currents, torque and speed with time are presented and compared with those obtained from previously published results to validate the simulation process.

Key words: Matrix converter, induction motor, Matlab/Simulink, variation, currents, torque

INTRODUCTION

Traditionally, rectifier/inverter systems are used with the induction motor drive system (Trzynadlowski, 2001) to control the motor speed. Recently, matrix converter which is a direct AC-AC converter has become a good alternative to the rectifier/inverter topology because of several advantages (Abdel-Halim *et al.*, 2011; Vargas *et al.*, 2009, 2010). Several researchers have presented the simulation of the matrix converter/induction motor system using Matlab/Simulink (Altun and Sunter, 2003; Imayavaramban *et al.*, 2006). However either the transfer ratio was calculated using a m-file in Matlab (Imayavaramban *et al.*, 2006) or using a simplified solution algorithm (Altun and Sunter, 2003). In Abdel-Halim *et al.* (2011), the matrix converter was simulated using Matlab/Simulink when the converter is loaded only with an inductive static load.

In this study, a matrix converter/induction motor system is modeled and then simulated in detail using Matlab/Simulink package when Venturini and Optimum Venturini Modulation Techniques (Wheeler *et al.*, 2002; Arevalo, 2008) are used.

MATERIALS AND METHODS

Matrix converter model: A simplified circuit arrangement of a nine-switch matrix converter system is shown in Fig. 1. In Fig. 1, an input filter is used to eliminate the higher order harmonics found in the input current and the clamp circuit shown in Fig. 1 is used for protection against overcurrent which occurs due to short circuit and against overvoltage which occurs due to open circuit (Imayavaramban *et al.*, 2006). The mathematical model of

the matrix converter will be represented by its output voltages and input currents. These voltages and currents are expressed in terms of switching functions, S of the converter switches. These switching functions are defined as follows (Huber and Borojevic, 1995; Wheeler *et al.*, 2002):

$$S_{kj} = \begin{cases} 1, & \text{switch } S_{kj} \text{ closed} \\ 0, & \text{switch } S_{kj} \text{ open} \end{cases}$$

$$K = \{A, B, C\}, j = \{a, b, c\}$$

The output voltages and input currents of the matrix converter can thus be obtained in terms of the switching functions from (Huber and Borojevic, 1995; Wheeler *et al.*, 2002):

$$\begin{bmatrix} v_a(t) \\ v_b(t) \\ v_c(t) \end{bmatrix} = \begin{bmatrix} S_{Aa}(t) & S_{Ba}(t) & S_{Ca}(t) \\ S_{Ab}(t) & S_{Bb}(t) & S_{Cb}(t) \\ S_{Ac}(t) & S_{Bc}(t) & S_{Cc}(t) \end{bmatrix} \begin{bmatrix} v_A(t) \\ v_B(t) \\ v_C(t) \end{bmatrix} \quad (1)$$

and:

$$\begin{bmatrix} i_A(t) \\ i_B(t) \\ i_C(t) \end{bmatrix} = \begin{bmatrix} S_{Aa}(t) & S_{Ab}(t) & S_{Ac}(t) \\ S_{Ba}(t) & S_{Bb}(t) & S_{Bc}(t) \\ S_{Ca}(t) & S_{Cb}(t) & S_{Cc}(t) \end{bmatrix} \begin{bmatrix} i_a(t) \\ i_b(t) \\ i_c(t) \end{bmatrix} \quad (2)$$

There are two constraints that should be taken into consideration during the matrix converter operation; these are (Huber and Borojevic, 1995; Wheeler *et al.*, 2002):

- Short circuit between the converter input terminals should be avoided
- Any output phase must never be open-circuited

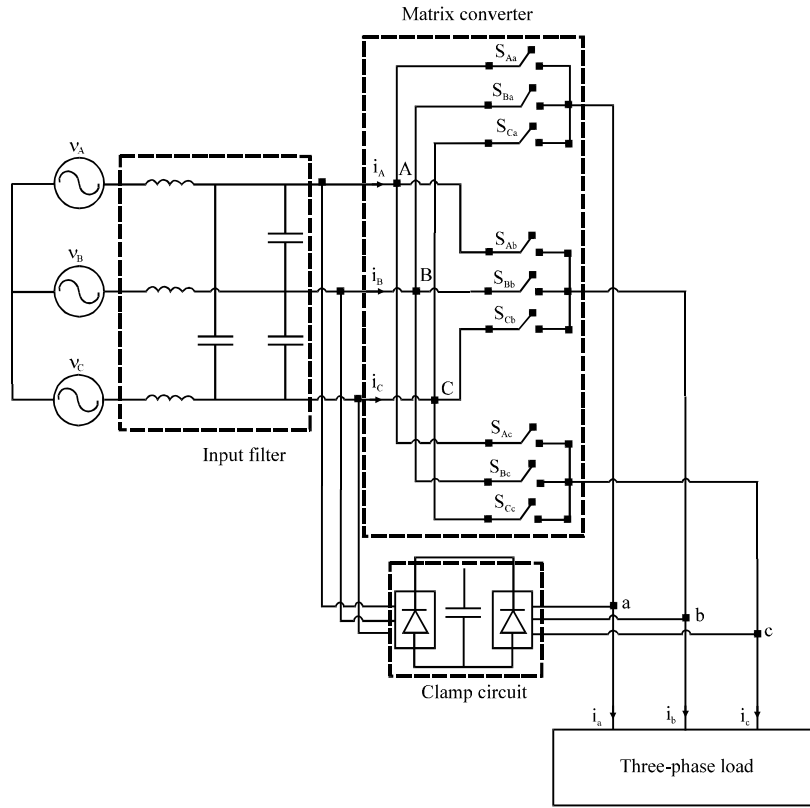


Fig. 1: Simplified circuit arrangement of a matrix converter system

These two constraints can be expressed mathematically in terms of the converter switching functions by Huber and Borjojevic (1995) and Wheeler *et al.* (2002):

$$S_{Aj} + S_{Bj} + S_{Cj} = 1, j = \{a, b, c\}$$

The pattern of the switching functions is based on the selected switching pattern. Figure 2 shows a typical switching pattern (Wheeler *et al.*, 2002). When the matrix converter switches are operated at a high switching frequency, low frequency output voltages can be obtained by controlling these switches according to certain modulation strategy (Alesina and Venturini, 1981, 1989; Arevalo, 2008; Huber and Borjojevic, 1995; Imayavaramban *et al.*, 2006; Shepherd and Zhang, 2004; Wheeler *et al.*, 2002).

In order to avoid high harmonic content in the output voltages of the matrix converter, the switching frequency must be >20 times the output frequency (Imayavaramban *et al.*, 2006). The modulation duty cycles of the switches of the matrix converter can be expressed in matrix form which is called modulation matrix (Arevalo, 2008; Shepherd and Zhang, 2004) or transfer matrix (Wheeler *et al.*, 2002; Imayavaramban *et al.*, 2006) as:

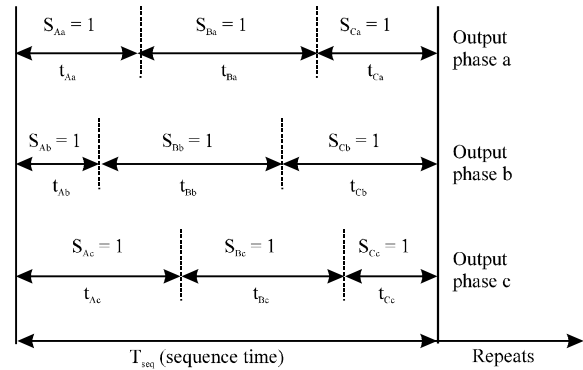


Fig. 2: General form of the switching pattern

$$M(t) = \begin{bmatrix} m_{Aa}(t) & m_{Ba}(t) & m_{Ca}(t) \\ m_{Ab}(t) & m_{Bb}(t) & m_{Cb}(t) \\ m_{Ac}(t) & m_{Bc}(t) & m_{Cc}(t) \end{bmatrix} \quad (3)$$

where:

$$m_{Kj}(t) = t_{Kj} / T_{seq} \quad (4)$$

The above mentioned constraints can be expressed mathematically in terms of the modulation duty cycles of the switches by Alesina and

Venturini (1981, 1989), Imayavaramban *et al.* (2006) and Wheeler *et al.* (2002):

$$\sum_{K=A,B,C} m_{K_a}(t) = \sum_{K=A,B,C} m_{K_b}(t) = \sum_{K=A,B,C} m_{K_c}(t) = 1 \quad (5)$$

The modulation duty cycles can be obtained using the Venturini and Optimum Venturini Methods (Arevalo, 2008; Wheeler *et al.*, 2002). The Venturini Method is used when the voltage gain ratio, q which is the ratio between output and input voltage is ≤ 0.5 . The following compact form is used for unity input displacement factor to obtain the modulation duty cycles in the considered range of q (Arevalo, 2008; Wheeler *et al.*, 2002):

$$m_{K_j} = \frac{t_{K_j}}{T_{seq}} = \frac{1}{3} \left(1 + \frac{2v_K v_j}{V_{im}^2} \right) \quad (6)$$

for:

$$K = \{A, B, C\}, \quad j = \{a, b, c\}$$

where, v_K refers to the input voltages which are given by:

$$v_i = V_{im} \begin{bmatrix} \cos(\omega_1 t) \\ \cos(\omega_1 t + 2\pi/3) \\ \cos(\omega_1 t + 4\pi/3) \end{bmatrix} \quad (7)$$

and v_j refers to the reference output voltages which are given by:

$$v_o = qV_{im} \begin{bmatrix} \cos(\omega_0 t) \\ \cos(\omega_0 t + 2\pi/3) \\ \cos(\omega_0 t + 4\pi/3) \end{bmatrix} \quad (8)$$

The optimum Venturini Method is used when the voltage gain ratio, q is > 0.5 and is $< \sqrt{3}/2$. In this case, the following compact form is used for unity input displacement factor, to obtain the modulation duty cycles in the considered range of q (Arevalo, 2008; Wheeler *et al.*, 2002):

$$m_{K_j} = \frac{1}{3} \left[1 + \frac{2v_K v_j}{V_{im}^2} + \frac{4q}{3\sqrt{3}} \sin(\omega_1 t + \beta_K) \right] \sin(3\omega_1 t) \quad (9)$$

for $K = A, B, C, j = \{a, b, c\}, \beta_K = 0, 2\pi/3, 4\pi/3$ for $K = A, B, C$, respectively. The reference output voltages, v_j in this case takes the following from (Alesina and Venturini, 1989; Arevalo, 2008; Imayavaramban *et al.*, 2006; Wheeler *et al.*, 2002):

$$v_o = qV_{im} \begin{bmatrix} \cos(\omega_0 t) - \frac{1}{6} \cos(3\omega_0 t) + \frac{1}{2\sqrt{3}} \cos(3\omega_1 t) \\ \cos(\omega_0 t + 2\pi/3) - \frac{1}{6} \cos(3\omega_0 t) + \frac{1}{2\sqrt{3}} \cos(3\omega_1 t) \\ \cos(\omega_0 t + 4\pi/3) - \frac{1}{6} \cos(3\omega_0 t) + \frac{1}{2\sqrt{3}} \cos(3\omega_1 t) \end{bmatrix} \quad (10)$$

Induction motor model: The induction motor will be modeled in terms of its d-q quantities in stationary reference frame. In this reference frame, a model in which the inversion of the inductance matrix of the motor equation is avoided will be used. Thus the motor electrical differential equation is (Abdel-Halim, 1979):

$$D[i] = \sigma\{[vL] + [RL].[i] + \omega_{me}[GL].[i]\} \quad (11)$$

where:

$$[i] = [i_{ds} \quad i_{qs} \quad i_{dr} \quad i_{qr}]^T$$

$$[vL] = [v_{ds}L_r \quad v_{qs}L_r \quad -v_{ds}M \quad -v_{qs}M]^T$$

$$[RL] = \begin{bmatrix} -R_sL_r & 0 & MR_r & 0 \\ 0 & -R_sL_r & 0 & MR_r \\ MR_s & 0 & -R_rL_s & 0 \\ 0 & MR_s & 0 & -R_rL_s \end{bmatrix}$$

$$[GL] = \begin{bmatrix} 0 & M^2 & 0 & ML_r \\ -M^2 & 0 & -ML_r & 0 \\ 0 & -ML_s & 0 & -L_sL_r \\ ML_s & 0 & L_rL_s & 0 \end{bmatrix}$$

$$\sigma = \frac{1}{L_rL_s - M^2}$$

Where:

- R_s = The stator resistance per phase
- R_r = The rotor resistance per phase referred to stator
- M = The mutual inductance per phase
- L_s = The stator self inductance per phase
- L_r = The rotor self inductance per phase referred to stator
- D = The operator d/dt
- ω_{me} = The rotor speed in elec.rad/sec
- i_{dr} and i_{qr} = The rotor direct and quadrature currents in the stationary reference frame
- v_{ds} and v_{qs} = The stator direct and quadrature voltages, respectively

The stator direct and quadrature voltages (v_{ds} and v_{qs}) in Eq. 11 are obtained from the three-phase stator voltages as (Sun *et al.*, 2005; Trzynadlowski, 2001):

$$\begin{bmatrix} v_{ds} \\ v_{qs} \end{bmatrix} = \frac{\sqrt{2}}{\sqrt{3}} \begin{bmatrix} 1 & -\frac{1}{2} & -\frac{1}{2} \\ 0 & \frac{\sqrt{3}}{2} & -\frac{\sqrt{3}}{2} \end{bmatrix} \begin{bmatrix} v_{as} \\ v_{bs} \\ v_{cs} \end{bmatrix} \quad (12)$$

The stator three-phase currents (i_{as} - i_{cs}) can also be obtained in terms of the stator d-q currents (i_{ds} and i_{qs}) from (Sun *et al.*, 2005; Trzynadlowski, 2001):

$$\begin{bmatrix} i_{as} \\ i_{bs} \\ i_{cs} \end{bmatrix} = \frac{\sqrt{2}}{\sqrt{3}} \begin{bmatrix} 1 & 0 \\ -\frac{1}{2} & \frac{\sqrt{3}}{2} \\ \frac{1}{2} & -\frac{\sqrt{3}}{2} \end{bmatrix} \begin{bmatrix} i_{ds} \\ i_{qs} \end{bmatrix} \quad (13)$$

The induction motor electromagnetic torque can be obtained in terms of the d-q currents in stationary reference frame from (Sun *et al.*, 2005; Trzynadlowski, 2001):

$$T_e = p.M.[i_{dr}.i_{qs} - i_{qr}.i_{ds}] \quad (14)$$

Method of analysis: The system will be investigated for certain values of voltage gain ratio, q output frequency, fo unity input power factor and input voltages, Eq. 7 as follows. The reference output voltages are obtained from Eq. 8 when voltage gain ratio is ≤ 0.5 . The modulation duty cycles are obtained from Eq. 6 using the obtained reference output voltages and given input voltages. When the value of the voltage gain ratio is:

$$0.5 \leq q \leq \frac{\sqrt{3}}{2}$$

The reference output voltages are obtained from Eq. 10. In this case, the modulation duty cycles of the matrix converter switches are obtained from Eq. 9 using the obtained reference output voltages and the given input voltages.

The conduction periods of the switches can thus be obtained during a s switching interval using the calculated modulation duty cycles. If the switching pattern shown in Fig. 2 is used, the switching functions can thus be obtained.

The switching functions can also be obtained by comparing the modulation duty cycles of the switches with a sawtooth waveform (Imayavaramban *et al.*, 2006). The amplitude of the sawtooth waveform is unity and its frequency equals to the switching frequency. The 3-phase output voltages of the matrix converter can be

obtained from Eq. 1 using the switching functions and the given input voltages. These voltages are transformed to d-q stationary reference frame using Eq. 12 to obtain v_{ds} and v_{qs} . These voltages are used in the motor electrical equation, Eq. 11. When the variation of the motor speed is taken into consideration during the transient period, Eq. 11 becomes nonlinear and numerical solution to obtain the motor currents is required. For this purpose, the motor mechanical equation is used at each step of simulation. The induction motor mechanical equation is given by (Abdel-Halim, 1979):

$$D\omega_m = \frac{T_e - T_l(\omega_m)}{J} \quad (15)$$

Where:

ω_m = The motor speed in rad/sec

J = The moment of inertia of the motor and its load

$T_l(\omega_m)$ = Motor total load torque which is given by:

$$T_l(\omega_m) = T_L + T_{fw}$$

Where:

T_L = The load torque

T_{fw} = The friction and windage torque. The electromagnetic torque

T_e = Obtained from Eq. 14

In order to obtain the actual values of the motor currents, a transformation from d-q to 3-phase quantities is performed. This is achieved using Eq. 13 for the currents i_{as} - i_{cs} , respectively. The corresponding input currents can be obtained, using Eq. 2 replacing i_a - i_c by i_{as} - i_{cs} , respectively.

SYSTEM SIMULATION

Simulation is achieved for the system under consideration using Matlab/Simulink software package. The overall Simulink block diagram of the system under consideration is shown in Fig. 3.

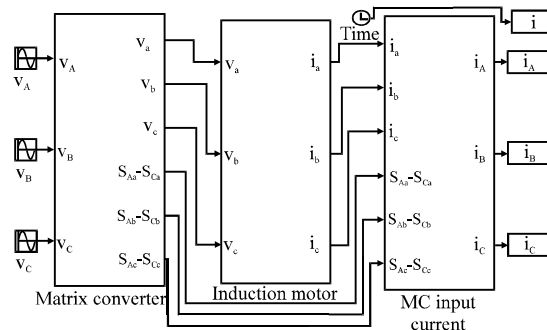


Fig. 3: System Simulink block diagram

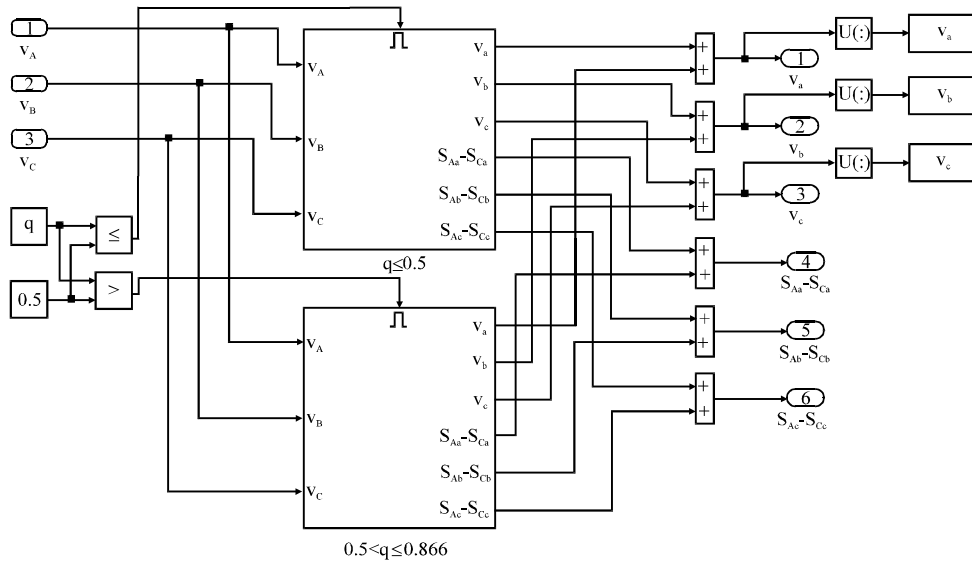


Fig. 4: Subsystem matrix converter

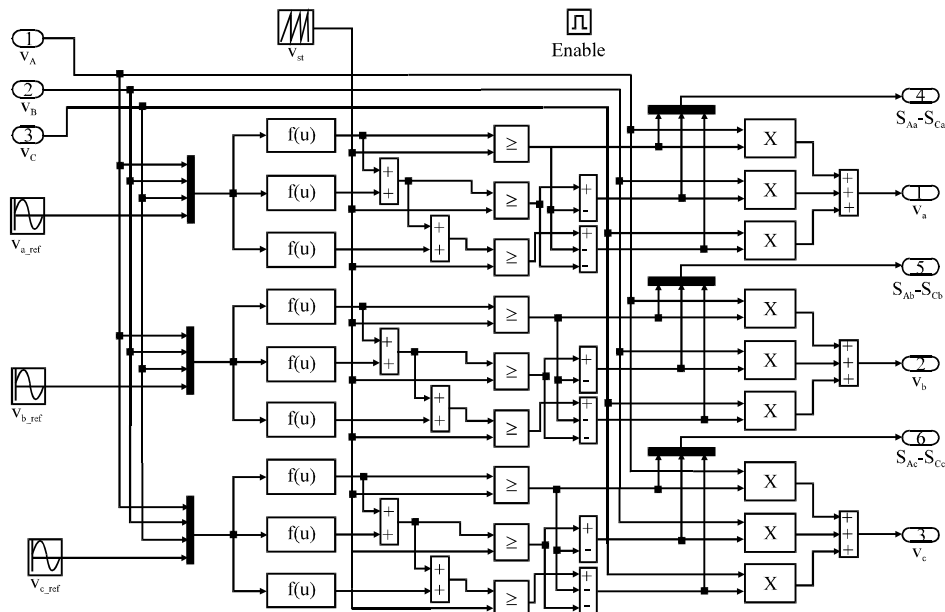


Fig. 5: Subsystem $q \leq 0.5$

It consists of three subsystems. They are matrix converter, induction motor and MC input current. The blocks v_A-v_C are used to represent the input voltage waveforms which are shown in Eq. 7.

The subsystem matrix converter is shown in Fig. 4 (Abdel-Halim *et al.*, 2011). It contains two subsystems which are called $q \leq 0.5$ and $0.5 < q \leq 0.866$. These subsystems are shown in Fig. 5 and 6, respectively. The block labeled in Fig. 5 and 6, v_{st} represents the sawtooth waveform and the block labeled enable is used to enable the subsystem output to be used when its input equals to

unity otherwise the output will be disabled. Figure 5 shows Eq. 1, 6 and 8. Figure 6 shows Eq. 1, 9 and 10. The details of the subsystem induction motor are shown in Fig. 7.

It consists of the subsystems voltage abc-dq transformation, IM mechanical and electrical equations and current dq-abc transformation. The details of the subsystem voltage abc-dq transformation are shown in Fig. 8. This subsystem shows Eq. 12. Figure 9 shows the details of the subsystem IM mechanical and electrical equations.

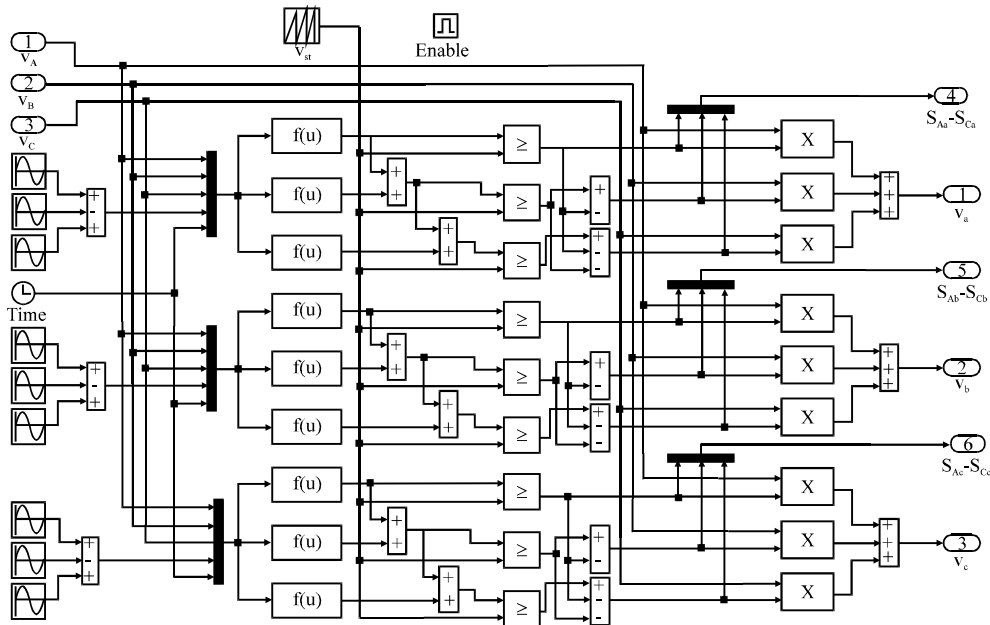


Fig. 6: Subsystem $0.5 < q \leq 0.866$

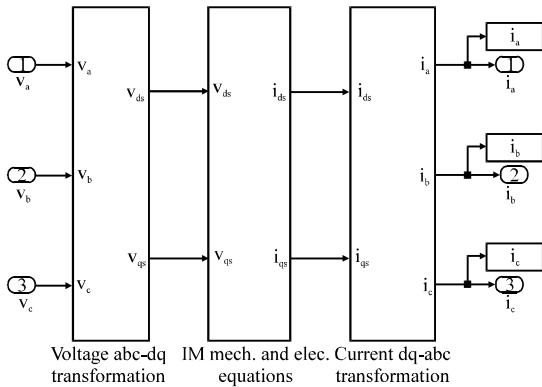


Fig. 7: Subsystem induction motor

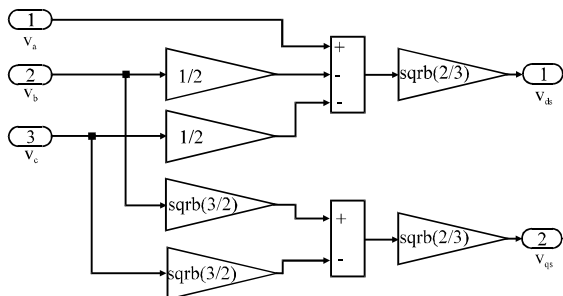


Fig. 8: Subsystem voltage abc-dq transformation

This subsystem represents the motor electrical and mechanical equations which are shown by Eq. 11, 14 and 15. It contains a subsystem named mechanical

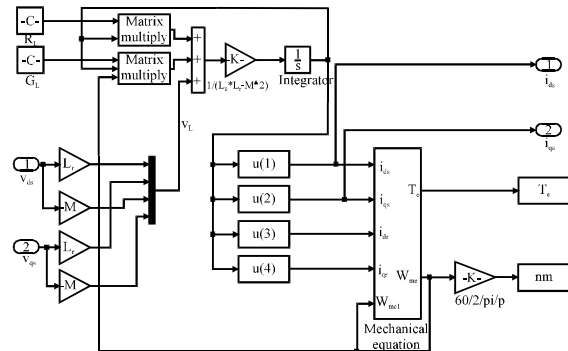


Fig. 9: The subsystem IM mechanical and electrical equations

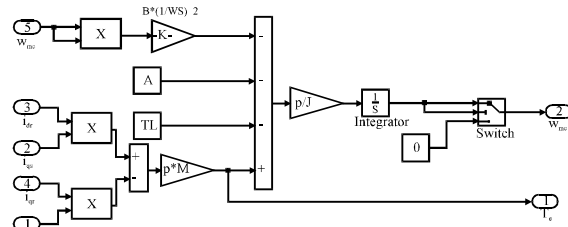


Fig. 10: The subsystem mechanical equations

equation whose details are shown in Fig. 10 and it shows Eq. 14 and 15. The details of the subsystem current dq-abc transformation are shown in Fig. 11. This subsystem shows Eq. 13. The details of the subsystem MC input current are shown in Fig. 12. It shows Eq. 2.

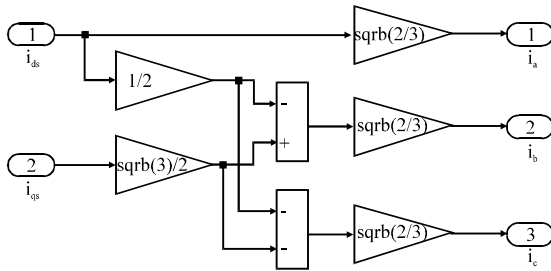


Fig. 11: The subsystem current dq-abc transformation

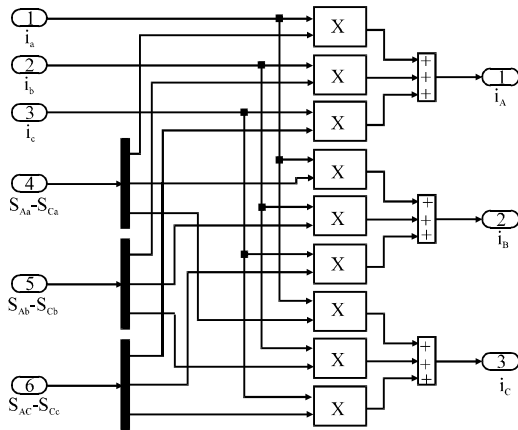


Fig. 12: Subsystem MC input current

RESULTS AND DISCUSSION

Several results are obtained using the simulation described above with the following data:

- Voltage gain ratio of the matrix converter: $q = 0.35$
- Peak value of the input voltage: $V_{im} = 327 \text{ V}$
- Output frequency: $f_o = 42 \text{ Hz}$
- Switching frequency: $f_s = 5 \text{ kHz}$

The data of the three-phase induction motor used in the system are shown in the Appendix. The induction motor is operated at no load. Figure 13 shows the three-phase output voltage waveforms of the matrix converter. Figure 14 shows the transient motor line current. The obtained line current is compared with that obtained in a published reference (Imayavaramban *et al.*, 2006) which is drawn (Fig. 14). It can be noticed from Fig. 14 that the compared results are almost identical which proves the validity of the constructed Matlab/Simulink block diagram. Figure 15 shows the steady-state motor line current. It can be noticed from this figure the motor current is approximately sinusoidal and contains low harmonic content. Figure 16 shows the transient motor torque. The steady-state motor torque is

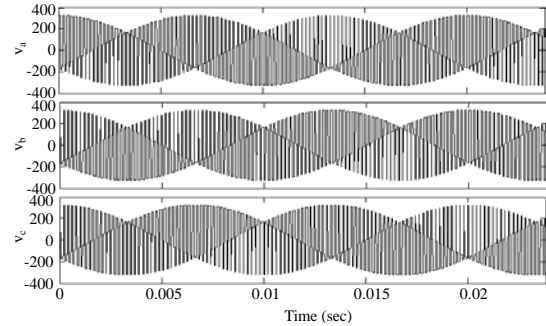


Fig. 13: 3-phase voltages output of the matrix converter when $q = 0.35$, $V_{im} = 327 \text{ V}$, $f_o = 42 \text{ Hz}$ and $f_s = 5 \text{ kHz}$

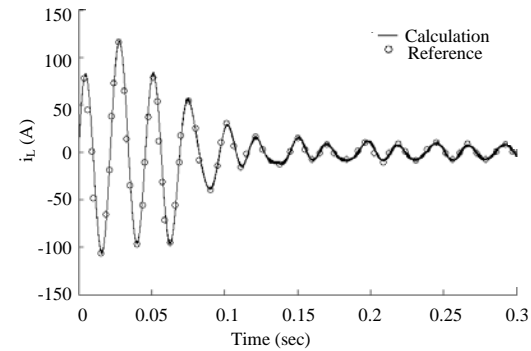


Fig. 14: Transient motor line current when $q = 0.35$, $V_{im} = 327 \text{ V}$, $f_o = 42 \text{ Hz}$ and $f_s = 5 \text{ kHz}$

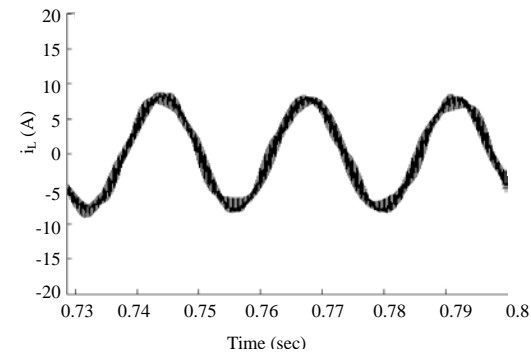


Fig. 15: Steady-state motor line current when $q = 0.35$, $V_{im} = 327 \text{ V}$, $f_o = 42 \text{ Hz}$ and $f_s = 5 \text{ kHz}$

shown in Fig. 17. It can be noticed from Fig. 17 that the torque contains oscillations. Figure 18 shows the motor transient speed. Results from the published reference (Imayavaramban *et al.*, 2006) are drawn in Fig. 18. It is noted that the obtained and the results of the reference are almost identical which again proves the validity of the simulation process. The steady-state motor speed is shown in Fig. 19. It is noticed from Fig. 19 that the speed contains very small oscillations which are due

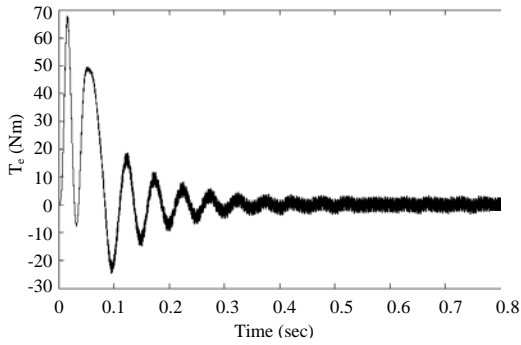


Fig. 16: Transient motor torque when $q = 0.35$, $V_{im} = 327$ V, $f_o = 42$ Hz and $f_s = 5$ kHz

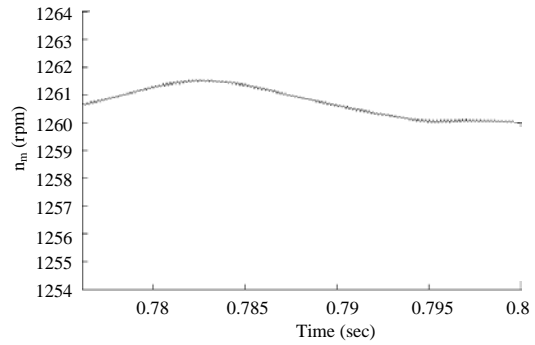


Fig. 19: Steady-state motor speed when $q = 0.35$, $V_{im} = 327$ V, $f_o = 42$ Hz and $f_s = 5$ kHz

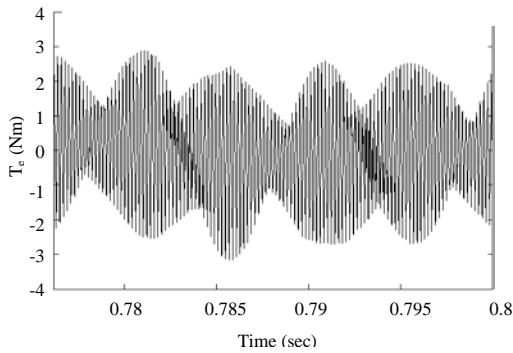


Fig. 17: Steady-state motor torque when $q = 0.35$, $V_{im} = 327$ V, $f_o = 42$ Hz and $f_s = 5$ kHz

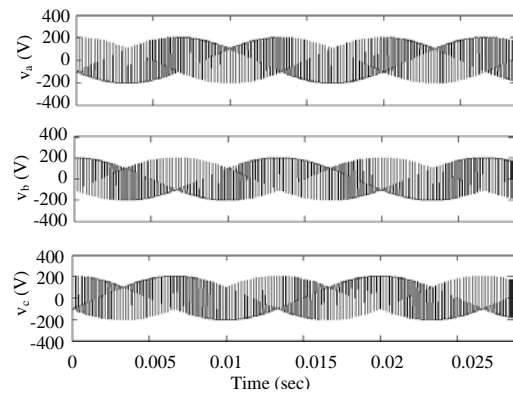


Fig. 20: Three-phase voltages output of the matrix converter when $q = 0.8$, $V_{im} = 204$ V, $f_o = 70$ Hz and $f_s = 5$ kHz

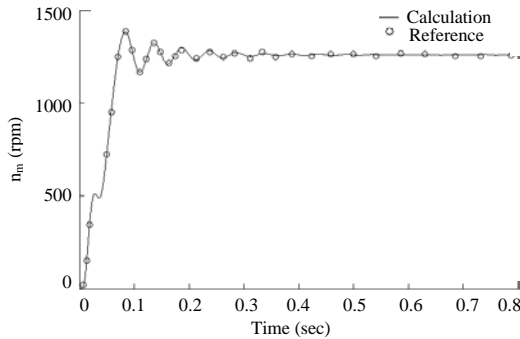


Fig. 18: Motor transient speed when $q = 0.35$, $V_{im} = 327$ V, $f_o = 42$ Hz and $f_s = 5$ kHz

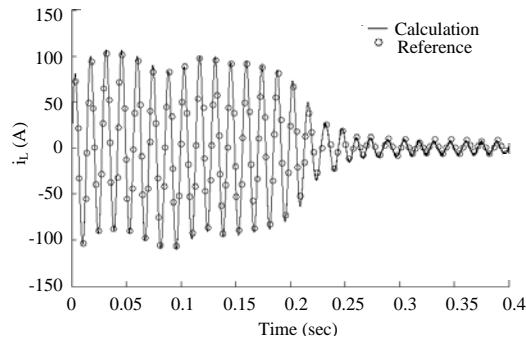


Fig. 21: Transient motor line current when $q = 0.8$, $V_{im} = 204$ V, $f_o = 70$ Hz and $f_s = 5$ kHz

to the torque oscillations shown in Fig. 17. Another set of results are obtained with the same switching frequency and the motor parameters and with the following data:

- Voltage gain ratio: $q = 0.8$
- Peak value of the input voltage: $V_{im} = 204$ V
- Output frequency: $f_o = 70$ Hz

Figure 20 shows the three-phase voltages output of the matrix converter for the case under consideration.

Figure 21 shows the transient motor line current. The obtained line current is compared with that obtained in reference (Imayavaramban *et al.*, 2006). It can be noticed from Fig. 21 that the two sets of results are almost identical. Figure 22 shows the steady-state motor line current. It can be noticed from Fig. 22, the motor current is approximately sinusoidal and contains harmonics. Figure 23 shows the transient motor torque. The steady-

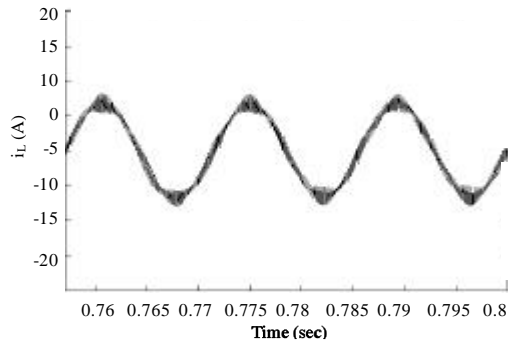


Fig. 22: Steady-state motor line current when $q = 0.8$, $V_{im} = 204$ V, $f_o = 70$ Hz and $f_s = 5$ kHz

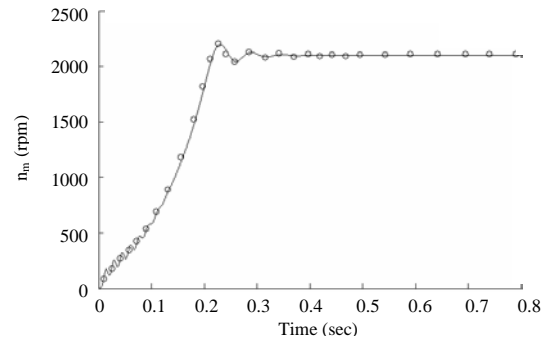


Fig. 25: Motor transient speed when $q = 0.8$, $V_{im} = 204$ V, $f_o = 70$ Hz and $f_s = 5$ kHz

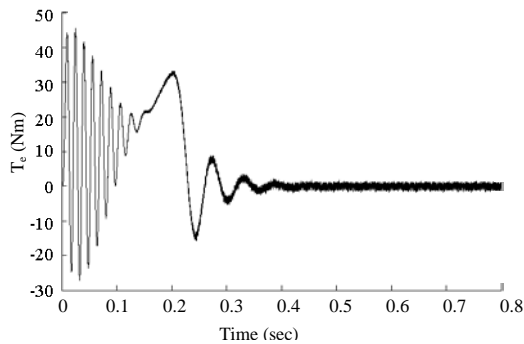


Fig. 23: Transient motor torque when $q = 0.8$, $V_{im} = 204$ V, $f_o = 70$ Hz, $f_s = 5$ kHz

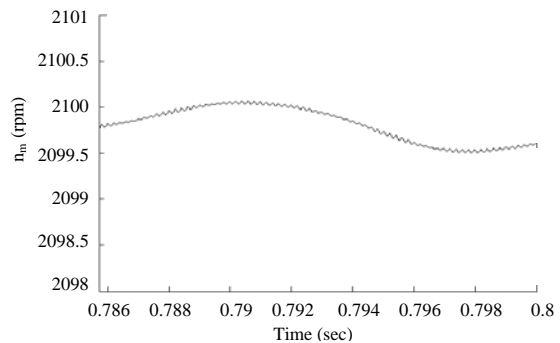


Fig. 26: Steady-state motor speed when $q = 0.8$, $V_{im} = 204$ V, $f_o = 70$ Hz and $f_s = 5$ kHz

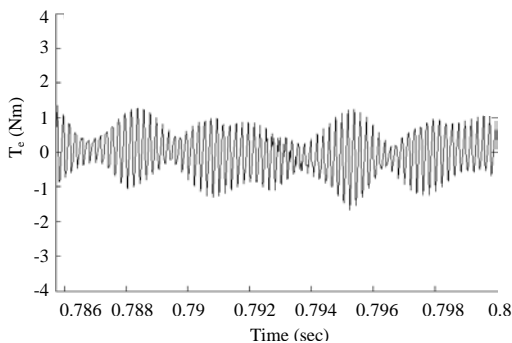


Fig. 24: Steady-state motor torque when $q = 0.8$, $V_{im} = 204$ V, $f_o = 70$ Hz and $f_s = 5$ kHz

state motor torque is shown in Fig. 24. It can be noticed from Fig. 24 that the torque contains oscillations. Figure 25 shows the motor transient speed. The obtained results are compared to those obtained from reference (Imayavaramban *et al.*, 2006). It can be noted that the results are almost identical. The steady-state motor speed is shown in Fig. 26. It can be noted from Fig. 26 that the speed contains very small oscillations due to the torque oscillations shown in Fig. 24.

CONCLUSION

A system composed of a matrix converter and a three-phase induction motor has been modeled and a Matlab/Simulink block diagram has been constructed in detail for it. The constructed block diagram for the matrix converter/induction motor system is used to study and analyze the performance of the system when the voltage gain ratio $q \leq 0.5$ and when $0.5 < q \leq 0.866$. The obtained results are almost identical with those obtained from previously published results which proves the validity of the simulation using Matlab/Simulink package.

APPENDIX

The parameters of the induction motor used in this system are: Three-phase, star-connected, 200 V, 60 Hz, 5 hp induction machine with (Imayavaramban *et al.*, 2006):

- $R_s = 0.277 \Omega$
- $L_s = 0.0553$ H
- $R_r = 0.183 \Omega$
- $L_r = 0.05606$ H
- $L_m = 0.0538$ H
- $J = 0.01667$ kg m⁻² and rated speed = 1766.9 rpm

REFERENCES

- Abdel-Halim, I.A.M., 1979. Modeling induction motors for computing transient behavior. *Proc. IEE*, 126: 343-344.
- Abdel-Halim, I.A.M., H.G. Hamed and A.M. Hassan, 2011. Modeling and simulation of a matrix converter/inductive load system. *Int. J. Electr. Power Eng.*, 5: 144-149.
- Alesina, A. and M. Venturini, 1981. Solid-state power conversion: A fourier analysis approach to generalized transformer synthesis. *IEEE Trans. Circuits Syst.*, 28: 319-330.
- Alesina, A. and M.G.B. Venturini, 1989. Analysis and design of optimum-amplitude nine switch direct AC-AC converters. *IEEE Trans. Power Electron.*, 4: 101-112.
- Altun, H. and S. Sunter, 2003. Matrix converter induction motor drive: Modelling, simulation and control. *Elect. Eng.*, 86: 25-33.
- Arevalo, S.L., 2008. Matrix converter for frequency changing power supply applications. Ph.D. Thesis, University of Nottingham.
- Huber, L. and D. Borojevic, 1995. Space vector modulated three-phase to three-phase matrix converter with input power factor correction. *IEEE Trans. Ind. Appl.*, 31: 1234-1246.
- Imayavaramban, M., A.V.K. Chaithanya and B.G. Fernandes, 2006. Analysis and mathematical modeling of matrix converter for adjustable speed AC drives. *Proceedings of the Power Systems Conference and Exposition*, October 29-November 1, 2006, Atlanta, GA., pp: 1113-1120.
- Shepherd, W. and L. Zhang, 2004. *Power Converters Circuits*. Marcel Dekker Inc., New York.
- Sun, F., J. Li, L. Sun, L. Zahi and F. Cguo, 2005. Modeling and simulation of vector control AC motor used by electric vehicle. *J. Asian Electr. Veh.*, 3: 669-672.
- Trzynadlowski, A.M., 2001. *Control of Induction Motors*. Academic Press, USA., ISBN: 9780127015101, Pages: 228.
- Vargas, R., U. Ammann and J. Rodriguez, 2009. Predictive approach to increase efficiency and reduce switching losses of matrix converters. *IEEE Trans. Power Electron.*, 24: 894-902.
- Vargas, R., U. Ammann, B. Hudoffsky, J. Rodriguez and P. Wheeler, 2010. Predictive torque control of an induction machine fed by a matrix converter with reactive input power control. *IEEE Trans. Power Electron.*, 25: 1426-1438.
- Wheeler, P.W., J. Rodriguez, J.C. Clare, L. Empringham and A. Weinstein, 2002. Matrix converters: A technology review. *IEEE Trans. Ind. Electron.*, 49: 276-288.